Pakistan Veterinary Journal

ISSN: 0253-8318 (PRINT), 2074-7764 (ONLINE)
Accessible at: www.pvj.com.pk

RESEARCH ARTICLE

Sequential Canine Neonatal Spinal Ultrasonography from Birth till Spinal Ossification

Mohammed S Amer, Elham A Hassan*, Faisal A Torad, Ashraf A Shamaa and Elsayed A Elsherpieny[1]

Department of Surgery, Anesthesiology and Radiology, Faculty of Veterinary Medicine, Cairo University, Giza, Egypt; [1]Department of Mathematical Statistics, Institute of Statistical Studies and Research, Cairo University, Giza, Egypt
*Corresponding author: elhamhassan@cu.edu.eg

ARTICLE HISTORY (15-068)

Received: February 08, 2015
Revised: May 11, 2015
Accepted: May 28, 2015
Online available: July 21, 2015

Key words:
Dog
Spinal canal
Spinal cord
Ultrasound

ABSTRACT

The purpose of this study was to report the normal ultrasonographic appearance and spinal cord sagittal diameter of canine neonates. Longitudinal and transverse scans were done on 11 clinically normal canine neonates were performed at 3, 10, 20 and 30 days of age, using 8-10 MHz linear transducer. Measurement of the spinal cord sagittal diameter was recorded at different spinal segments. The spinal cord was recognized as an anechoic to hypoechoic tubular structure within the spinal canal, the three meningeal layers enclosing the cord were identified as hyperechoic dura and pia matters with the anechoic subarachnoid matter in between the two. The spinal cord sagittal diameter at the cervical and lumbar regions was greater than that of the thoracic region, and the cord was tapered at the mid-lumbar region forming the conus medullaris. It was difficult to visualize the spinal cord after 30 days of age. In conclusion, ultrasonographic imaging of the canine neonatal spinal cord varies with age till 30 days old.

To Cite This Article: Amer MS, Hassan EA, Torad FA, Shamaa AA and Elsherpieny EA, 2016. Sequential canine neonatal spinal ultrasonography from birth till spinal ossification. Pak Vet J, 36(1): 6-10.

INTRODUCTION

Ultrasonography of the spine is a non-invasive method used for diagnosing spinal diseases in human neonates (Kawahara *et al*., 1987). The incompletely ossified posterior arches of infants's vertebrae act as acoustic window for visualizing the spinal canal (Rubin *et al*., 1988). In older ages, spinal ultrasonography can only be performed in cases of spina bifida or following laminectomy (Mankin *et al*., 2012).

The ultrasonographic appearance of the canine neonatal spinal cord has been described (Finn-Bodner *et al*., 1995; Schmidt *et al*., 2008). The technique allows accurate spinal imaging and characterization of spinal abnormalities within the first few days of life (Lowe *et al*., 2007). The diagnostic value of spinal ultrasonography includes its ability to diagnose congenital spinal malformation (myelomeningiocele, spinal lipoma, diastematomyelia and syringomyelia) and acquired diseases such as meningeal tears or spinal injury due to birth trauma (Braun *et al*., 1983). Spinal ultrasonography also provides the basis of accurate correlation between injury and segment level with subsequently effective treatment (Ko *et al*., 2004; Hecht *et al*., 2014).

Little literatures have been published describing the canine neonatal spinal ultrasonography. The purpose of the present study was to report the normal ultrasonographic appearance and sagittal diameter of normal canine neonatal spinal cord from birth till ossification of the spinous arches.

MATERIALS AND METHODS

The present study was carried out on 11 neonates (6 male and 5 female) of mixed-breed dogs. All study procedures were approved by Animal Care and Use Ethical Committee of Faculty of Veterinary Medicine, Cairo University, Egypt. Spinal ultrasonography was done at 3, 10, 20 and 30 days of age, using 8-10 MHz linear transducer attached to a Samsung Madison (SONOACE R3®-Korea) machine. An acoustic coupling gel was applied over the back. Puppies were held by assistant in ventral recumbency. The head and neck were kept horizontally in straight position with the back. The transducer was placed over the midline starting from the atlanto-occipital articulation and moved backward till the lumbo-sacral articulation. Care was taken to keep the puppies fixed in straight position to obtain exact midline images.

Longitudinal and transverse images were recorded at the upper and lower cervical, cranial and caudal thoracic, as well as cranial and caudal lumbar regions. The focal

zone, image resolution and time gain compensation were fixed before each examination. The appearance and diameter of the spinal cord were recorded along the spinal canal starting from the atlas (C_1) and ended at the last lumbar vertebra (L_7). Ultrasonographic detectability of the examined spinal segment was reported at the different regions based on previously established anatomical landmarks (Budras *et al*., 2007; Baines *et al*., 2009). Briefly, in cervical region, the second cervical vertebra (axis) was taken as a landmark. The first three thoracic vertebrae with their long spinous processes were taken as landmark for counting the cranial thoracic segments. In the caudal thoracic region, the anticlinal vertebra (T_{11}) with its vertically directed spinous process was taken as a landmark. In lumbar region, the anatomical landmark was taken from the transverse scan through detection of the last rib-bearing vertebra that presumed to be T_{12} and the sequential numbering was made (T_{13}- L_7).

Measurements were made on the exact mid-sagittal plane from the inner aspect of the hyperechoic dorsal and ventral pia matter, each measurement was made three times and the mean was calculated. All examinations were performed by the same examiner; data were stored digitally and analyzed offline.

Statistical analysis: The spinal cord diameter at the different segments was expressed as means ± SD. Data were analyzed using SPSS software 21 (IMP SPSS Inc., Chicago, IL). Wilcoxon Signed Rank Test was used for detection of statistically significant differences of the spinal sagittal diameter at different ages (3, 10, 20 and 30 days). The results were considered statistically significant at $P<0.05$.

RESULTS

In longitudinal scan, the spinal cord appeared as a well-defined anechoic to hypoechoic tubular structure within the spinal canal. The spinal cord at the cervical and lumbar regions was obviously wider than the thoracic region. The cord showed tapering at the mid-lumbar region (L_3- L_5), forming the conus medullaris.

At 3 days of age:

In longitudinal scans, the spinal cord was as a well-defined anechoic tubular structure within the cervical and thoracic regions, while in the lumbar region it was anechoic to almost hypoechoic structure. The dura matter was identified as echogenic horizontal lines seen dorsal and ventral to the cord in the cervical and thoracic regions, while it was tightly adhered to the dorsal and ventral surfaces at the lumbar region. In cervical and lumbar regions, the pia matter was a thin echogenic linear structure, covering the cord parenchyma dorsally and ventrally, while it was visualized only ventrally in the thoracic region. The subarachnoid space within the cervical region (cisterna magna) was visualized in between the hyperechoic dura and pia matter as anechoic cerebrospinal fluid-filled space. In the thoracic and lumbar regions, the subarachnoid space was decreased to a narrow anechoic line along the spinal canal (Figs 1 and 2).

Fig. 1: Longitudinal scan of the cervical (C) spinal cord segment at 3-days of age. Note the anechoic tubular spinal cord (SC), the hyperechoic pia matter (PM), the anechoic subarachnoid space (SA) and the hyperechoic dura matter (DM).

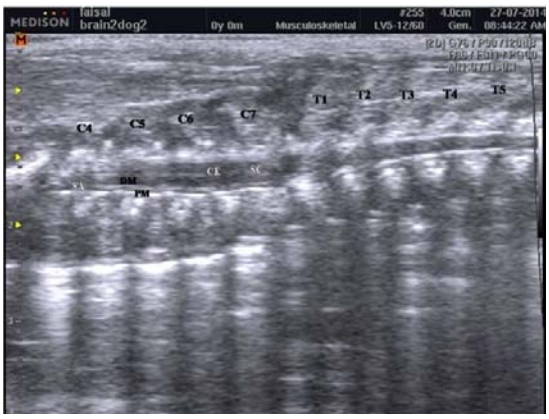

Fig. 2: Longitudinal scan of the cervico-thoracic spinal cord segment at 3-days of age. Note the hyperechoic pia matter (PM), the anechoic subarachnoid space (SA) and the hyperechoic dura matter (DM), the short cranially directed cervical vertebrae (C) and the long caudally directed spinous process of the thoracic vertebrae (T). The diameter of the spinal cord at the cervical region is greater than that of the thoracic region. The hypoechoic central echoes (CE) divide the anechoic spinal cord (SC).

Fig. 3: Transverse scan of the cervical spinal cord segment at 3-days of age. The spinal cord is anechoic spheroid structure is centrally positioned within the spinal canal. The dura matter and the pia matter could not be differentiated.

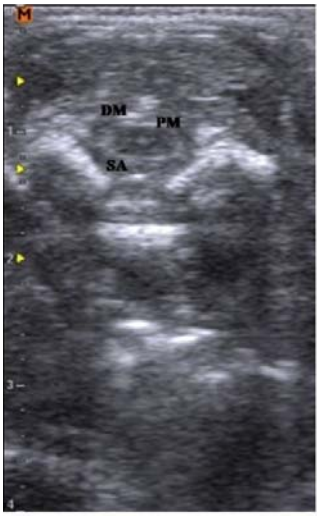

Fig. 4: Transverse scan of the thoracic spinal cord segment at 10-days of age. The spinal cord is mild heterogeneous ovoid structure with few echogenic foci. The dura matter (DM), pia matter (PM) and the subarachnoid space (SA) could be easily differentiated.

Fig. 5: Transverse scan of the lumbar spinal cord segment at 10-days of age. The spinal cord is heterogeneous ovoid structure with few echogenic foci. The dura matter (DM), pia matter (PM) and the subarachnoid space (SA) could be easily differentiated. Note the transverse process (TP) of the lumbar vertebrae.

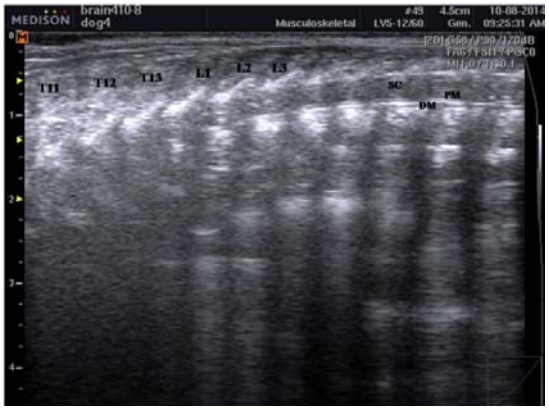

Fig. 6: Longitudinal scan of the thoraco-lumbar spinal cord segment at 20-days of age. Note the tubular heteroechoic appearance of the spinal cord (SC) with multiple echogenic focci and enclosed by the hyper echoic pia matter (PM) and dura matter (DM).

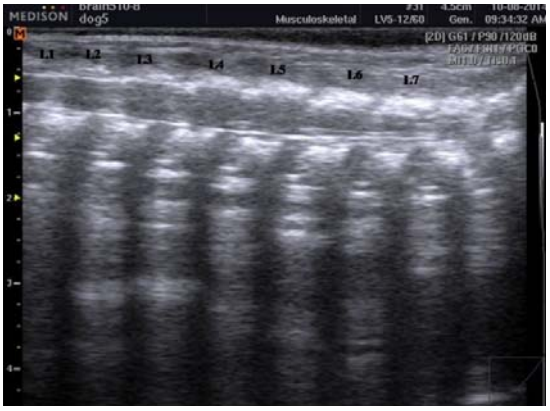

Fig. 7: Longitudinal scan of the lumbar (L) spinal cord segment at 20-days of age. Tapering of the spinal cord starting from the L4 forming the conus medullaris. The hyperechoic dura and pia matter are clearly differentiated.

In transverse scans, the spinal cord was spheroid (in the cervical region), ovoid (in the thoracic region) or round (in the lumbar region) anechoic structure surrounded by hyperechoic pia matter. The dura matter was closely adhering to the spinal canal in the cervical region, while the pia and dura matter could not be differentiated at the thoracic and lumbar regions (Fig 3).

At 10 days of age*:*

In longitudinal scans, the spinal cord in the cervical region was anechoic to hypoechoic. A linear central echo was seen near the middle of the cord; this central echo was unequally dividing the cord parenchyma into narrow dorsal and wide ventral parts. In the thoracic region, cord was a mildly heterogenic structure with few echogenic foci, while in the lumbar region it was more heterogenic with multiple echogenic foci along its parenchyma. The hyperechoic dura and pia matters were more echogenic and more thick than they were at 3 days of age.

In transverse scans, the spinal cord was mildly heterogeneous ovoid structure with few echogenic focci at the cervical and thoracic regions. However, in the lumbar region, multiple echogenic foci were seen within the heterogenic cord parenchyma. The hyperechoic dura and pia matters could be differentiated enclosing the anechoic subarachnoid space (Figs 4 and 5).

At 20 days of age:

In longitudinal scans, the spinal cord was uniformly tubular hypoechoic structure with homogenous less echogenic central echo along its segments. The largest diameter of the cord was recorded at C_6 - C_7. The diameter of the cord was almost equal along the thoracic segment (Figs 6 and 7).

In transverse scans, the spinal cord was elliptical heterogenic structure in the cervical region and ovoid hypoechoic structure in both thoracic and lumbar regions with central echogenic foci.

At 30 days of age:

In longitudinal and transverse scans, the appearance of the spinal cord and its surrounding meninges was similar

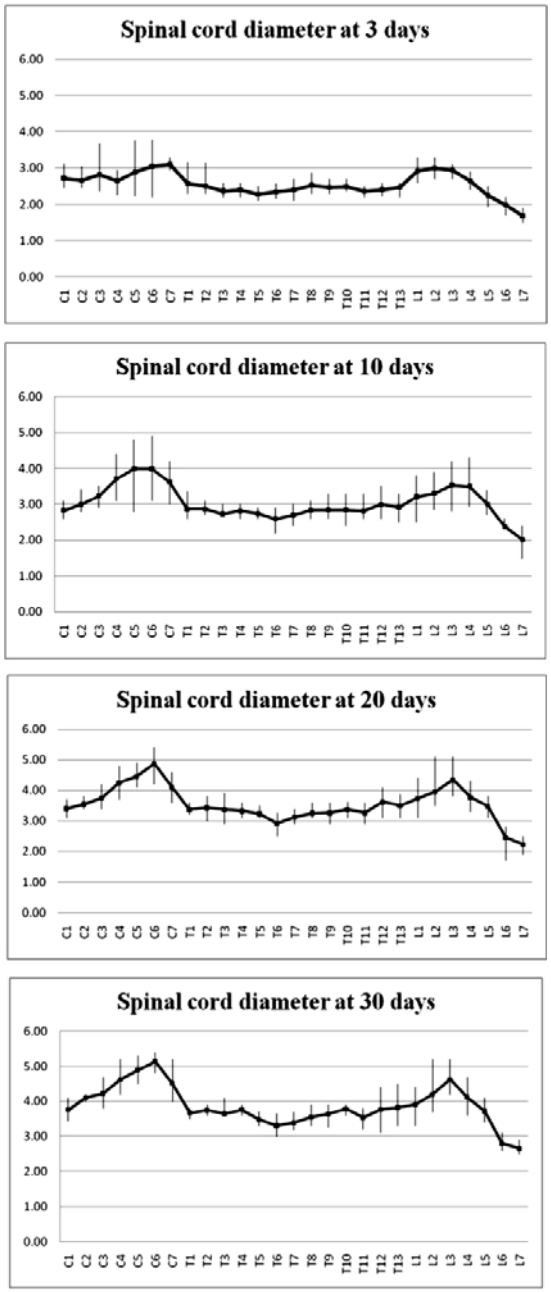

Fig. 8: The mean measurements of the spinal cord sagittal diameter (mm) at 3, 10, 20 and 30 days of age at different spinal cord segments.

to that of the 20 days of age. It was difficult to visualize the cord after 30 days of age, as ossification of the spinous processes hindered the ultrasonographic examination.

The sagittal diameter of the spinal cord was significantly increased with age at all examination times except C_1 between 3 and 10 days, L_1 and L_6 between 20 and 30 days as well as L_4 between 10 and 20 days. The mean measurements of spinal cord sagittal diameter at the different ages are presented in Fig 8.

DISCUSSION

The spinal cord was recognized as anechoic to hypoechoic tubular structure within the spinal canal surrounded by three meningeal layers including the hyperechoic dura and pia matter and the anechoic subarachnoid matter. The echogenicity of dura matter was stronger than the pia matter which may be due to presence of dense longitudinally oriented bundles of collagen, elastic fibers as well as flattened fibroblasts (Budras *et al*., 2007; Baines *et al*., 2009). The subarachnoid space appeared anechoic between the dura-arachnoid layers and the surface of spinal cord as it is filled with acellular cerebrospinal fluid (Beltran *et al*., 2012). Detection of dorsal and ventral subarachnoid space depends on the amount of cerebrospinal fluid which varies according to the region visualized (Evans and Christensen, 1979). It has been reported that the dorsal and ventral borders of the spinal cord were echogenic due to the difference in acoustic impedance between subarachnoid space and spinal cord parenchyma (Nakayama, 1993). In our opinion, the echogenic appearance of dorsal and ventral borders of the spinal cord could be attributed to the closely adhered dorsal and ventral pia matter. The echogenic appearance of the pia matter seems to be due to its collagen and elastic fibers as well as longitudinally oriented fibroblasts (Budras *et al*., 2007). Moreover, the acoustic enhancement produced by the cerebrospinal fluid in the subarachnoid space may participate in the echogenic appearance of the cord.

The parenchymal echogenicity of the spinal cord varied with age of neonates from anechoic (3 days old), mild heteroechogenic (10 days of age), heteroechogenic (20 days of age) to homogenous hypoechoic (30 days of age). The increased echogenicity could be attributed to the increased fiber tracts or parenchymal vasculature (Teele and Share, 1991; Nakayama, 1993). The grey matter with its few myelinated nerve fibers could not be differentiated from the densely myelinated white matter using the 8-10 MHz transducer, which is similar to a previous study (Teele and Share, 1991).

Obvious variation was noticed in the sagittal diameter of the spinal cord at the cervical and lumbar levels compared to the diameter at the thoracic level. It has been reported that the cervical and lumbar intumescences may be due to the increased nerve fibers required for the formation of the brachial and lumbosacral plexus respectively (Zalel *et al*., 2006; Lowe *et al*., 2007).

Limitations of the present study included the use of relatively low number of animals of only one breed and the absence of Magnetic Resonance Imaging or autopsy study parallel to the ultrasound examination. In conclusion, the neonatal spinous processes can be used as an acoustic window for visualizing the spinal cord and its adjacent structures during the first month of life. The spinal cord is a well-defined anechoic to almost hypoechoic tubular structure within the spinal canal. The size and echogenicity of the spinal cord parenchyma increase with the age of neonates.

REFERENCES

Baines EA, Grandage J, Herrtage ME and Baines SJ, 2009. Radiogralphic definition of the anticlinal vertebra in the dog. Vet Radiol Ultrasound, 50: 69-73.

Beltran E, Dennis R, Doyle V, de Stefani A, Holloway A and de Risio L, 2012. Clinical and magnetic resonance imaging features of canine compressive cervical myelopathy with suspected hydrated nucleus pulposus extrusion. J Small Anim Pract, 53: 101-107.

Braun IF, Raghavendra BN and Kricheff II, 1983. Spinal cord imaging using real-time high-resolution ultrasound. Radiology, 147: 459-465.

Budras K, McCarthy P, Fricke W and Richter R, 2007. Anatomy of the Dog. Schlütersche Verlagsgesellschaftmb H& Co. KG, Hans-Böckler-Allee, Hannover, Germany.

Evans H and Christensen G, 1979. Spinal cord and meninges. In: Millers Anatomy of the Dog. 2ed Ed. WB Saunders Company, Philadelphia, USA.

Finn-Bodner S, Hudson JA, Coates JR, Sorjonen DC, Simpson ST, Cox NR, Wright JC, Garrett PD, Steiss JE, Vaughn DM, Miller SC and Brown SA, 1995. Ultrasonographic anatomy of the normal canine spinal cord and correlation with histopathology after induced spinal cord trauma. Vet Radiol Ultrasound, 36: 39-48.

Hecht S, Huerta MM and Reed RB, 2014. Magnetic resonance imaging (MRI) spinal cord and canal measurements in normal dogs. Anat Histol Embryol, 43: 36-41.

Kawahara H, Andou Y, Takashima S, Takeshita K and Maeda K, 1987. Normal development of the spinal cord in neonates and infants seen on ultrasonography. Neuroradiology, 29: 50-52.

Ko HY, Park JH, Shin YB and Baek SY, 2004. Gross quantitative measurements of spinal cord segments in human. Spinal Cord, 42: 35-40.

Lowe LH, Johanek AJ and Moore CW, 2007. Sonography of the neonatal spine: Part 2, Spinal disorders. Am J Roentgenol, 188: 739-744.

Mankin JM, Hecht S and Thomas WB, 2012. Agreement between T2 and haste sequences in the evaluation of thoracolumbar intervertebral disc disease in dogs. Vet Radiol Ultrasound, 53: 162-166.

Nakayama M, 1993. Intraoperative spinal ultrasonography in dogs: Normal findings and case-history reports. Vet Radiol Ultrasound, 34: 264-268.

Rubin JM, Di Pietro MA, Chandler WF and Venes J, 1988. Spinal ultrasonography: Intraoperative and pediatric applications. Radiol Clin North Am 26: 1- 27.

Schmidt MJ, Wigger A, Jawinski S, Golla T and Kramer M, 2008. Ultrasonographic appearance of the craniocervical Junction in normal brachycephalic dogs and dogs with Caudal occipital (chiari-like) malformation. Vet Radiol Ultrasound, 49: 472-476.

Teele R and Share J, 1991. Spinal ultrasonography and intraoperative neurosonography. In: Bralow I (ed), Ultrasonography of Infants and Children. WB Saunders Company, Philadelphia, USA.

Zalel Y, Lehavi O, Aizenstein O and Achiron R, 2006. Development of the fetal spinal cord: time of ascendance of the normal conus medullaris as detected by sonography. J Ultrasound Med, 25: 1397-1401.